Asian Journal of Water, Environment and Pollution. Vol. 22, No. 6 (2025), pp. 210-220.
doi: 10.36922/AJWEP025260210

ORIGINAL RESEARCH ARTICLE

Assessment of the surface urban heat island in Ho Chi Minh City using remote sensing and geographic information systems

Lam Van Hao[1,2]*

[1]Department of Oceanology, Meteorology and Hydrology, Faculty of Physics and Engineering Physics, University of Science, Ho Chi Minh, Vietnam
[2]Viet Nam National University-Ho Chi Minh City, Ho Chi Minh, Vietnam
***Corresponding author:** Lam Van Hao (lvhao@hcmus.edu.vn)

Received: June 26, 2025; Revised: July 10, 2025; Accepted: July 15, 2025; Published online: October 3, 2025

Abstract: The rapid urbanization of Ho Chi Minh City (HCMC) has led to an increasingly intense urban heat island (UHI) phenomenon, significantly impacting its environment and inhabitants. This study investigates the spatiotemporal dynamics of the surface UHI (SUHI) in HCMC by utilizing a 36-year time series of Landsat satellite imagery (1988, 1995, 2002, 2010, 2017, and 2024), processed within a geographic information system framework. Land surface temperature (LST) was derived to map and quantify UHI patterns. The results reveal a substantial and progressive intensification of the SUHI effect, with the citywide mean LST increasing from 25.4°C in 1988 to 28.7°C in 2024. Spatially, the SUHI has expanded from the urban core into peripheral suburban zones, particularly toward the east and northwest. A strong and consistent negative correlation ($R^2 > 0.7$) was observed between LST and the normalized difference vegetation index, underscoring the critical role of green spaces in mitigating urban heat. These findings provide crucial, data-driven insights for urban planners and policymakers, highlighting the urgent need for sustainable development strategies—such as enhancing green infrastructure and adopting cool materials—to combat the adverse effects of urban warming in this rapidly expanding tropical metropolis.

Keywords: Geographic information system; Land surface temperature; Landsat; Remote sensing; Urban heat island

1. Introduction

Urbanization is a defining global trend of the 21st century, characterized by the migration of populations to urban centers and the consequent expansion of urban land cover.[1] While this process often drives economic growth, it concurrently induces significant environmental modifications, one of the most prominent being the urban heat island (UHI) effect.[2,3] The UHI phenomenon describes the tendency for urban areas to experience higher atmospheric and surface temperatures than their surrounding rural and undeveloped counterparts.[4]

This thermal disparity is primarily attributed to alterations in the urban surface energy balance. The replacement of natural landscapes with impervious surfaces (e.g., concrete, asphalt) results in lower albedo (reflectivity) and higher thermal admittance, causing more solar energy to be absorbed and stored.[5] This is compounded by reduced evapotranspirational cooling due to diminished vegetation cover, complex urban geometry that traps solar radiation, and anthropogenic heat emissions from buildings, transportation, and industrial activities.[6,7] When referring specifically to surface temperature anomalies observed by remote sensors, the phenomenon is termed surface urban heat island (SUHI).

Conventionally, UHI studies relied on *in situ* air temperature measurements from fixed weather stations.[8] While valuable, this approach often suffers from sparse station networks, limiting its ability to capture the fine-scale spatial heterogeneity of urban thermal environments.[9] Remote sensing technology offers a powerful alternative, providing synoptic, spatially continuous data over large urban expanses with frequent revisit capabilities.[10] Satellite-derived land surface temperature (LST) is a key parameter for SUHI studies, enabling the detailed mapping and monitoring of thermal patterns.[9] The Landsat series of satellites, with its long-term archive and moderate-resolution thermal infrared bands, has been used extensively for LST retrieval and SUHI analysis globally.[11,12] Concurrently, the normalized difference vegetation index (NDVI), another standard satellite-derived product, is used to quantify vegetation density and assess its cooling effect.[13]

Numerous studies have investigated the SUHI phenomenon across diverse urban settings. For instance, research in Bangkok, Thailand, using Landsat 8 imagery, revealed that LST in urban areas was typically 4°C higher than in vegetated suburban areas.[14] Similar investigations in other Asian megacities, such as Shenzhen, China, and New Delhi, India, have also reported significant SUHI effects, with urban LST exceeding that of vegetated areas by 3–4°C and correlating strongly with land use changes and impervious surface expansion.[15,16] These studies underscore the commonality of the SUHI phenomenon while also highlighting the city-specific nature of its intensity and drivers, which are influenced by local geography, climate, and urban form. Ho Chi Minh City (HCMC), Vietnam's largest urban agglomeration and primary economic engine, has undergone exceptionally rapid urbanization over recent decades.[17] With a population exceeding 10 million, this growth has involved a significant transformation of agricultural land into built-up areas, accompanied by extensive infrastructure development.[18] Such land use/land cover (LULC) changes have inevitably impacted the local climate, contributing to the emergence and intensification of the SUHI phenomenon in HCMC.[19,20] Previous research has provided a valuable foundation for understanding this issue. However, a continuous, multi-decadal assessment incorporating the most recent data is needed to fully understand long-term trends and inform effective mitigation strategies.

The novelty and primary contribution of this study lie in its unprecedented temporal scale. By employing a consistent methodology across a 36-year time series from 1988 to 2024, this research provides the most comprehensive long-term assessment of SUHI dynamics in HCMC to date. This multi-decadal approach allows us not only to confirm the existence of SUHI but also to meticulously quantify its evolution, expansion, and changing intensity over time, an insight unattainable from shorter-term studies. This deep historical perspective is critical for developing far-sighted urban planning policies and effective climate change adaptation strategies.

This study aims to contribute to this understanding by: (i) Assessing the spatiotemporal evolution of the SUHI phenomenon in HCMC using a 36-year time series of Landsat imagery (1988–2024); (ii) quantifying LST changes across the urban-rural gradient to analyze the expansion and intensification of the heat island; and (iii) investigating the correlation between LST and NDVI to quantitatively evaluate the role of vegetation in modulating surface temperatures. The findings are expected to provide a comprehensive, updated perspective on SUHI dynamics in HCMC, offering crucial, data-driven insights for urban planners and policymakers to develop effective strategies for sustainable urban development and climate change adaptation.

2. Materials and methods

2.1. Study area

HCMC, located in the southeastern region of Vietnam, is the nation's largest city and a primary economic, cultural, and educational hub. Characterized by substantial growth and urban expansion, the city covers a total area of approximately 2,095 km^2 (Figure 1). HCMC's topography is generally flat, with about 60% of its area lying below an average elevation of 1.0 m. The city experiences a tropical monsoon climate with distinct wet (May–November) and dry (December–April) seasons. The population has grown to over 9 million residents, with an average density of 4,481 people/km^2, and approximately 80% residing in urbanized areas.[18] The rapid and often unplanned urban sprawl has led to significant alterations in land use, contributing to environmental challenges, including the SUHI effect.

2.2. Data collection and pre-processing

This study utilized multi-temporal Landsat satellite imagery from Landsat 5 Thematic Mapper (TM), Landsat 7 Enhanced TM Plus (ETM+), and Landsat 8 Operational Land Imager/Thermal Infrared Sensor.

Cloud-free or minimally clouded scenes covering HCMC for the years 1988, 1995, 2002, 2010, 2017, and 2024 were acquired from the United States Geological Survey Earth Explorer portal.[21] Detailed information on the acquired imagery is presented in Table 1.

Standard pre-processing steps, including radiometric calibration, were performed. For the Landsat 7 ETM+ image acquired after the scan line corrector failure in May 2003, a gap-filling technique using local histogram matching was applied to correct data gaps. Vector data

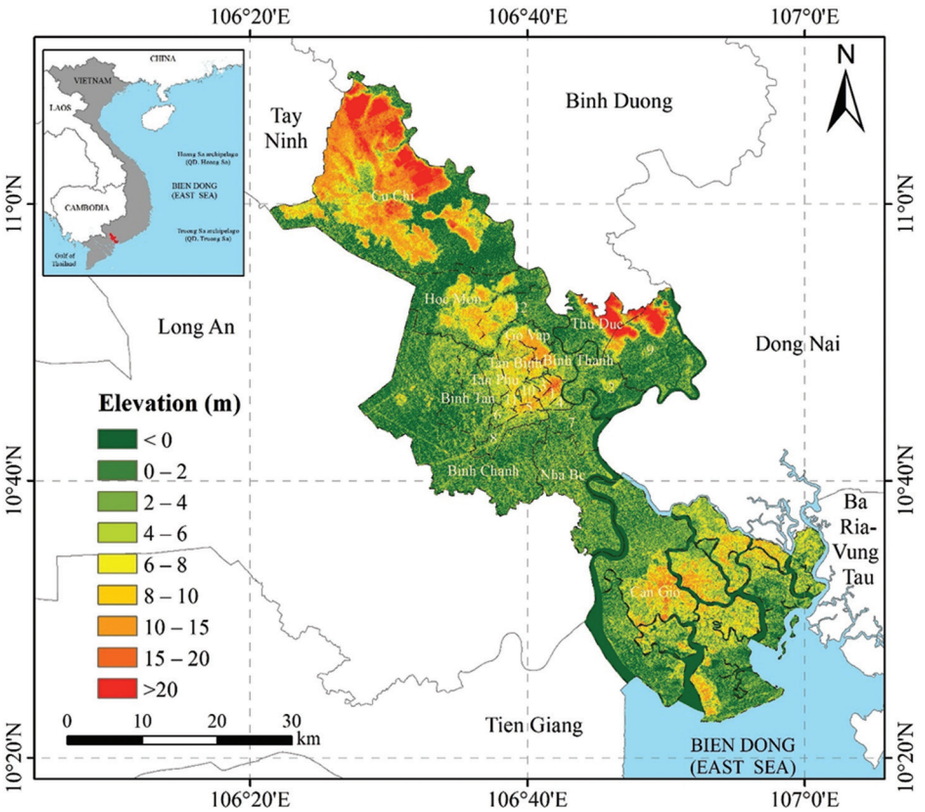

Figure 1. Elevation map of the study area in Ho Chi Minh City

Table 1. Satellite image data used in the study

Sensor	Path/row	Date of acquisition	Cloud coverage (%)	Spatial resolution (m)
Landsat 5 TM	125/053	January 14, 1988	11.00	30
Landsat 5 TM	125/052	January 14, 1988	0.00	30
Landsat 5 TM	125/053	February 02, 1995	5.00	30
Landsat 5 TM	125/052	February 02, 1995	0.00	30
Landsat 7 ETM+	125/053	February 13, 2002	18.00	30
Landsat 7 ETM+	125/052	February 13, 2002	5.00	30
Landsat 5 TM	125/053	February 11, 2010	43.00	30
Landsat 5 TM	125/052	February 11, 2010	1.00	30
Landsat 8 OLI/TIRS	125/053	February 14, 2017	14.75	30
Landsat 8 OLI/TIRS	125/052	February 14, 2017	0.52	30
Landsat 8 OLI/TIRS	125/053	February 18, 2024	22.92	30
Landsat 8 OLI/TIRS	125/052	February 18, 2024	0.06	30

Abbreviations: ETM+: Enhanced thematic mapper plus; OLI: Operational land imager; TIRS: Thermal infrared sensor; TM: Thematic mapper.

defining the administrative boundaries of HCMC were obtained from local government sources and used to delineate the study area.

2.3. Data processing and analysis

All image processing was conducted using established remote sensing algorithms listed below. The overall research workflow is illustrated in Figure 2.

(i) Radiance and reflectance: Digital numbers from level 1 products were converted to at-sensor spectral radiance (L^{λ}) and then to top-of-atmosphere planetary reflectance (ρ^{λ}), using the scaling factors and formulas provided in the image metadata and the Landsat Data Users Handbooks.[22,23] For Landsat 5/7/8, this included a correction for the solar elevation angle.

(ii) NDVI: NDVI was calculated using the reflectance of the red and near-infrared (NIR) bands, as per Equation I:

$$NDVI = \frac{\rho_{Nir} - \rho_{Red}}{\rho_{Nir} + \rho_{Red}} \quad (I)$$

(iii) Land surface emissivity (ε): Land surface emissivity was estimated based on the NDVI-threshold method described by Sobrino *et al*.[9] which assigns emissivity values according to NDVI to differentiate between soil, vegetation, and mixed pixels.

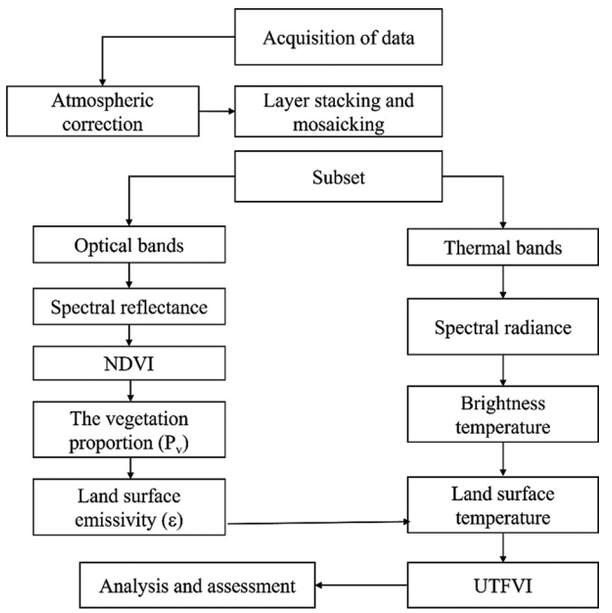

Figure 2. Flowchart of the research methodology, illustrating the process from data acquisition to surface urban heat island analysis

Abbreviations: NDVI: Normalized difference vegetation index; UTFVI: Urban thermal field variance index.

$$\varepsilon = \begin{cases} 0.979 - 0.035_{Red} & NDVI < NDVI_{Min} \\ 0.986 + 0.004P_V & NDVI_{Min} \le NDVI \le NDVI_{Max} \\ 0.99 & NDVI > NDVI_{Max} \end{cases} \quad (II)$$

where P_v is determined from the following formula[13]:

$$P_V = \left[\frac{NDVI - NDVI_{Min}}{NDVI_{Max} - NDVI_{Min}} \right]^2 \quad (III)$$

with $NDVI_{Max} = 0.5$, $NDVI_{Min} = 0.2$.

(iv) LST: First, at-sensor brightness temperature (T_B) was derived from the thermal band's spectral radiance using Planck's law inversion with metadata-provided constants. LST was then calculated in Celsius by correcting T_B for land surface emissivity using the following equation[24,25]:

$$LST\,(C) = \frac{T_B}{1 + \left(T_B / \alpha \right) \ln(\varepsilon)} - 273.15 \quad (IV)$$

where λ is the wavelength of the emitted radiance, and $\alpha = hc/k$ (1.438×10^{-2} mK).

(v) Urban thermal field variance index (UTFVI): The UTFVI is used to assess the SUHI effect based on LST and is divided into six levels of ecological evaluation (Table 2). It is calculated using Equation V[26-28]:

$$UTFVI = \frac{LST - LST_m}{LST_m} \quad (V)$$

where LST is the land surface temperature of each pixel, and LST_m is the mean land surface temperature of the study area.

2.4. SUHI assessment and accuracy

To comprehensively evaluate the characteristics and reliability of the SUHI patterns derived in this study, the following analytical steps were undertaken.

(i) SUHI classification and analysis: The generated LST maps were classified into distinct thermal zones to facilitate analysis. Thresholds were defined based on the overall temperature distribution for each year to represent relative thermal conditions: Low (<26°C), moderate (26–30°C), high (30–34°C), and very high (>34°C). The spatiotemporal trends, intensity, and expansion of the SUHI were assessed through qualitative map comparison, calculation of citywide mean LST, and analysis of mean LST across concentric buffer zones (5, 10, 15, and 30 km radii) from the city center.

(ii) Accuracy assessment: While a full quantitative accuracy assessment using a confusion matrix was

not performed due to the lack of contemporaneous, high-resolution ground-truth temperature data for all historical years, the reliability of the results is supported by several factors. The LST retrieval methods are standardized and widely validated in the scientific literature. Furthermore, the strong and physically consistent correlation observed between LST and NDVI provides confidence in the generated thermal patterns.

(iii) Correlation analysis: The relationship between LST and NDVI was quantified using Pearson's correlation coefficient (R) and the coefficient of determination (R^2) for pixels with positive NDVI values.

3. Results

3.1. Spatiotemporal distribution of the SUHI

The spatial distribution of LST across HCMC from 1988 to 2024 consistently reveals pronounced SUHI characteristics (Figures 3-5). Higher LST values are predominantly concentrated in industrial zones and densely built-up urban districts, where impervious surfaces dominate. Conversely, lower LST values are observed in areas with extensive green cover, such as the agricultural lands of Hoc Mon and Cu Chi, and the Can Gio mangrove forest.

In 1988 (Figure 3A), the highest LST values (30–32°C) were largely confined to the core urban districts. By 1995 (Figure 3B), high LST zones (>30°C) became more widespread, expanding into surrounding areas. This trend of intensification and spatial expansion continued through 2002 and 2010 (Figure 4), as well as 2017 and 2024 (Figure 5), with the highest temperature zones progressively encroaching on formerly cooler suburban areas. The general trend indicates an increasing proportion of the city area experiencing higher LST values, while areas with low LST are diminishing.

Table 2. Threshold values of UTFVI and corresponding ecological evaluation categories

UTFVI	LST-LST$_m$ (°C)	SUHI phenomenon	Ecological evaluation index
<0	<0	None	Excellent
0≤UTFVI<0.005	0≤LST–LSTm<1.5	Weak	Good
0.005≤UTFVI<0.010	1.5≤LST–LSTm<3.0	Middle	Normal
0.010≤UTFVI<0.015	3.0≤LST–LSTm<4.5	Strong	Bad
0.015≤ UTFVI<0.020	4.5≤LST–LSTm<6.0	Stronger	Worse
UTFVI≥0.020	LST–LSTm≥6.0	Strongest	Worst

Abbreviations: LST: Land surface temperature of each pixel; LST$_m$: Mean land surface temperature; SUHI: Surface urban heat island; UTFVI: Urban thermal field variance index.

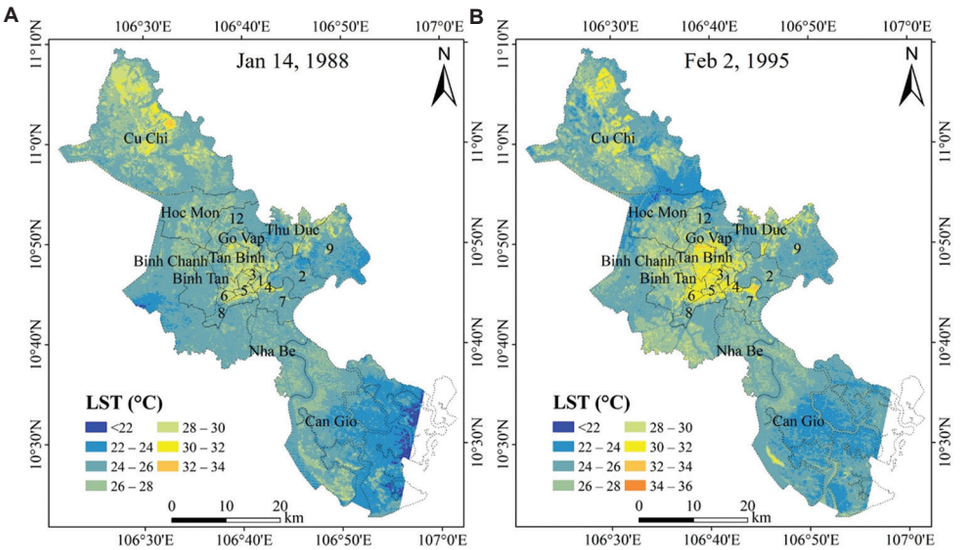

Figure 3. Spatiotemporal distribution of land surface temperature (LST) in Ho Chi Minh City in (A) 1988 and (B) 1995

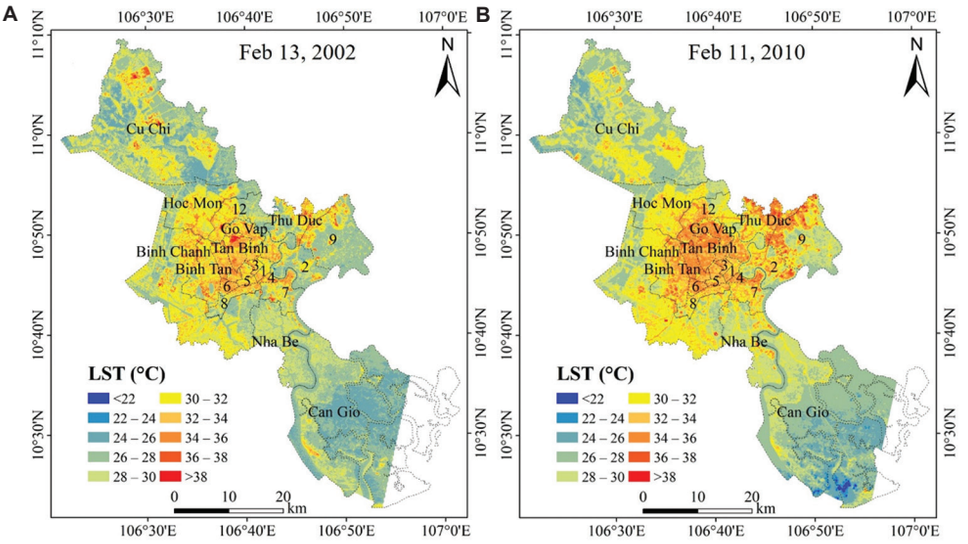

Figure 4. Spatiotemporal distribution of land surface temperature (LST) in Ho Chi Minh City in (A) 2002 and (B) 2010

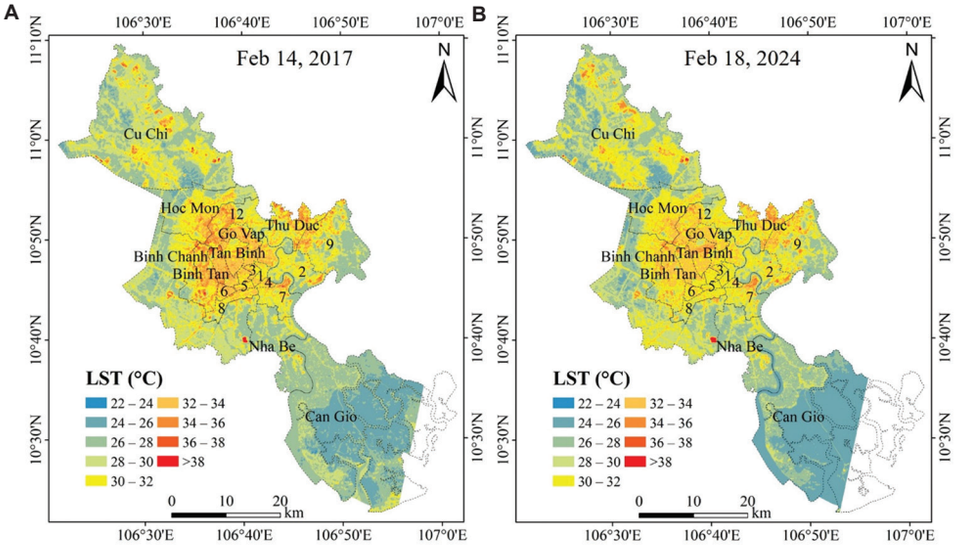

Figure 5. Spatiotemporal distribution of land surface temperature (LST) in Ho Chi Minh City in (A) 2017 and (B) 2024

3.2. Temporal trends and expansion of the UHI

The analysis of mean LST for the entire study area reveals a clear warming trend over the 36-year period (Figure 6). The mean LST for HCMC was 25.4°C in 1988, 25.2°C in 1995, 28.3°C in 2002, 29.4°C in 2010, 28.3°C in 2017 (a slight dip, potentially due to specific meteorological conditions), and 28.7°C in 2024.

To further quantify SUHI expansion, mean LST was analyzed across different distances from the city center (Table 3). The results consistently show that as the distance from the center increases, the mean LST decreases, which is characteristic of a classic UHI profile. The data also reveal a general increasing trend in mean LST at all distances over the 36-year period, with the most significant warming observed in the outer suburban zones. This indicates that the warming is not confined to the urban core but is a broader phenomenon affecting the entire metropolitan region.

3.3. Correlation between LST and NDVI

The relationship between LST and NDVI was investigated to assess the influence of vegetation on

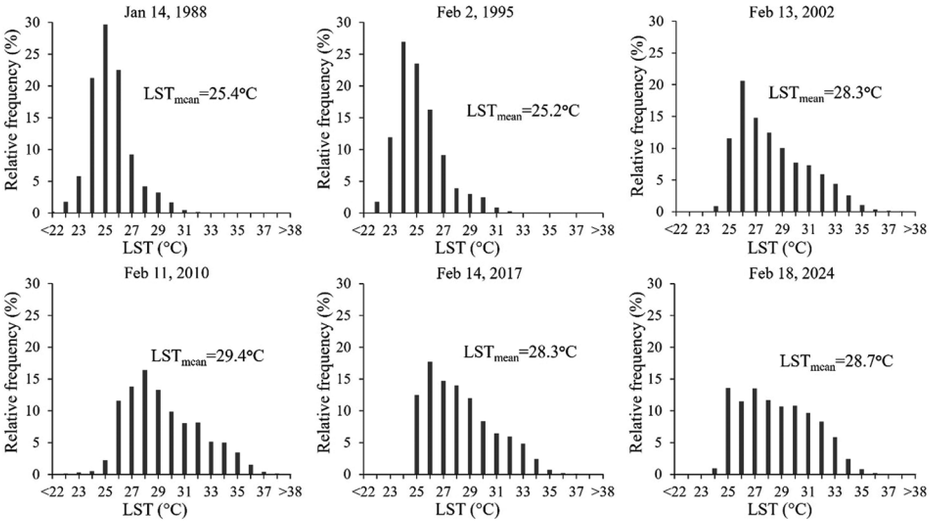

Figure 6. Temporal distribution of land surface temperature (LST) in Ho Chi Minh City from 1988 to 2024

Table 3. Mean land surface temperature (°C) in Ho Chi Minh City at varying distances from the city center (1988–2024), including percentage change

Radius (km)	1988 (°C)	Change (%)	1995 (°C)	Change (%)	2002 (°C)	Change (%)	2010 (°C)	Change (%)	2017 (°C)	Change (%)	2024 (°C)	Change (%)
5	27.4	0	28.9	0	32.5	0	34	0	31.6	0	32.1	0
10	26.1	−4.7	26.9	−6.9	30.9	−4.9	32.7	−3.8	30.8	−2.5	31.4	−2.2
15	25.6	−6.6	26.0	−10.0	29.9	−8.0	31.7	−6.8	29.6	−6.3	30.4	−5.3
30	25.4	−7.3	25.6	−11.4	29	−10.8	30.6	−10.0	28.6	−9.5	29.6	−7.8

surface temperatures. A consistent and strong negative correlation was observed for all analyzed years (Figure 7). The coefficient of determination (R^2) for this relationship was >0.7 in all years, signifying a robust inverse relationship. This indicates that areas with higher vegetation density (higher NDVI) consistently exhibit lower surface temperatures, while areas with sparse or no vegetation (lower NDVI) have higher LST. Detailed regression statistics are presented in Table 4.

Table 4. Regression statistics for the relationship between land surface temperature and normalized difference vegetation index

Year	*R*	R^2	Adjusted R^2	Standard error	*p*-value
1988	0.836	0.699	0.694	0.923	<0.05
1995	0.878	0.771	0.768	1.055	<0.05
2002	0.901	0.811	0.809	1.412	<0.05
2010	0.901	0.812	0.810	1.300	<0.05
2017	0.906	0.821	0.819	1.161	<0.05
2024	0.904	0.816	0.815	1.101	<0.05

4. Discussion

4.1. Spatiotemporal SUHI dynamics in HCMC

The results of this study clearly demonstrate the presence, intensification, and spatial expansion of the SUHI phenomenon in HCMC from 1988 to 2024. The observed patterns—higher LST in densely built-up urban cores and lower LST in vegetated suburban areas—are consistent with established SUHI characteristics reported in numerous cities worldwide.[29] The multi-temporal analysis revealed a substantial rise in mean LST across HCMC, from 25.4°C in 1988 to 28.7°C in 2024. This warming trend, coupled with the outward expansion of the heat island (as shown in Table 3 and Figures 3-5), is a direct consequence of rapid urbanization, the conversion of natural and agricultural land to impervious surfaces, and increased anthropogenic activities.[20]

4.2. Critical role of vegetation in SUHI mitigation

A key finding of this study is the strong and consistent negative correlation ($R^2 > 0.7$) between LST and NDVI.

This empirically validates the crucial role of vegetation in mitigating urban heat through evapotranspirational cooling and shading effects.[24,30] This finding has significant implications for urban planning in HCMC (Table 2). As the city continues to grow, the preservation and strategic integration of green infrastructure—such as parks, green roofs, urban forests, and vegetated corridors—becomes paramount for thermal regulation and for improving urban comfort and resilience.[31]

4.3. SUHI versus canopy layer UHI (CLUHI)

It is important to distinguish between the SUHI, measured by satellite-derived LST, and the CLUHI, measured by *in situ* air temperature at weather stations. SUHI reflects the temperature of surfaces (e.g., roads, rooftops), whereas CLUHI reflects the temperature of the air that people experience. SUHI typically exhibits a much greater thermal amplitude than CLUHI, with peak intensity during the daytime when urban surfaces strongly absorb solar radiation.[2] In contrast, CLUHI is often most intense at night, as urban areas release stored heat more slowly than rural surroundings (Table 5). Our study focuses on SUHI, which provides a spatially comprehensive view of how different land use types affect the surface energy balance, which is the fundamental driver of the entire UHI phenomenon.

4.4. Implications for urban planning and public health

The intensification of the SUHI in HCMC has several potential adverse consequences. These include increased energy demand for cooling, which can strain energy infrastructure and exacerbate greenhouse gas emissions[32]; a heightened risk of heat-related health problems for urban residents, such as heat stress and heat stroke[33]; and negative impacts on local ecosystems and air quality.[24] The expansion of the SUHI into suburban areas suggests that these previously less-affected regions

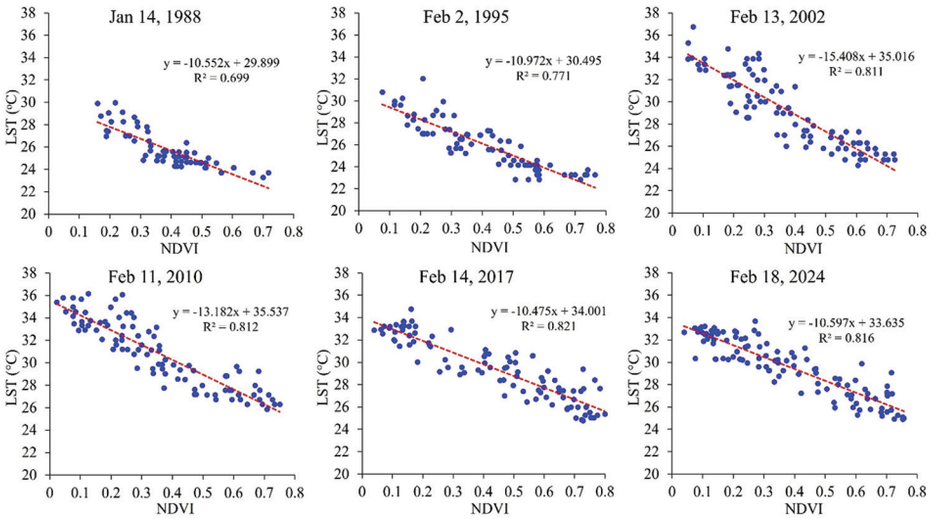

Figure 7. Scatter plots showing the correlation between LST and NDVI for selected years from 1988 to 2024
Abbreviations: LST: Land surface temperature; NDVI: Normalized difference vegetation index.

Table 5. Statistics of the surface UHI phenomenon based on the urban thermal field variance index

UHI phenomenon	Ecological evaluation index	1988		1995		2002		2010		2017		2024	
		ha	%	ha	%	ha	%	ha	%	ha	%	ha	%
None	Excellent	109,964	56.9	117,098	60.6	107,132	55.4	109,334	56.6	108,945	56.4	76,211	39.4
Weak	Good	54,126	28.0	43,019	22.3	27,323	14.1	29,722	15.4	33,972	17.6	30,695	15.9
Middle	Normal	18,213	9.4	18,111	9.4	20,177	10.4	23,129	12.0	20,665	10.7	29,579	15.3
Strong	Bad	7,965	4.1	10,028	5.2	15,698	8.1	15,332	7.9	17,043	8.8	25,088	13.0
Stronger	Worse	2,530	1.3	4,207	2.2	11,614	6.0	11,964	6.2	10,005	5.2	16,431	8.5
Strongest	Worst	436	0.2	1,076	0.6	4,133	2.1	4,146	2.1	2,543	1.3	4,977	2.6

Abbreviation: UHI: Urban heat island.

are becoming more vulnerable to heat stress, potentially impacting agricultural productivity and the well-being of suburban populations. Mitigation strategies are therefore imperative, including the promotion of "cool materials" (high-albedo roofs and pavements), enhancement of the urban tree canopy, and the design of shaded public spaces (Table 5).[34]

4.5. Limitations and future research

While this study provides valuable insights, certain limitations should be acknowledged. The use of Landsat imagery, while offering a good balance of spatial and temporal resolution, is susceptible to cloud cover, which can limit data availability in tropical regions. The LST retrieval algorithms, though widely accepted, involve certain assumptions that may introduce uncertainties. Furthermore, the spatial resolution of the thermal bands, though resampled to 30 m, is natively coarser and may not capture micro-scale thermal variations within complex urban structures. Critically, this study did not perform a detailed quantitative LULC change analysis, but rather illustrated such changes visually.

Future research could build upon these findings by: (i) Integrating higher-resolution thermal imagery (e.g., Advanced Spaceborne Thermal Emission and Reflection Radiometer, ECOsystem Spaceborne Thermal Radiometer Experiment on Space Station) to examine micro-scale SUHI variations; (ii) conducting a quantitative LULC change analysis to model its relationship with LST increases; (iii) incorporating 3D urban morphology data to develop more sophisticated models; and (iv) assessing the socio-economic impacts of SUHI on public health and energy consumption.

5. Conclusion

This study comprehensively assessed the spatiotemporal dynamics of the SUHI in HCMC over a 36-year period (1988–2024). The findings confirm that HCMC experiences a significant and intensifying SUHI effect, characterized by markedly higher LSTs in urbanized areas compared to surrounding rural regions. Our research demonstrated a substantial increase in the city's overall mean LST, from 25.4°C in 1988 to 28.7°C in 2024, with the thermal impacts of urbanization expanding from the urban core into previously cooler suburban areas. Furthermore, a strong and consistent negative correlation between LST and NDVI underscores the critical cooling role of vegetation.

The implications of these findings are significant for urban planning and environmental management. The documented intensification and expansion of the SUHI necessitate proactive measures to mitigate its adverse effects on human health, energy consumption, and urban livability. Strategies must prioritize the preservation and enhancement of green infrastructure, the adoption of cool construction materials, and the implementation of sustainable urban design principles to foster a more resilient and comfortable urban environment in HCMC.

Acknowledgments

The author expresses gratitude to the University of Science, Viet Nam National University- HCMC, for their support.

Funding

This research was funded by the University of Science, Viet Nam National University-HCMC, under grant number T2024-21.

Conflict of interest

The author declares no competing interests.

Author contributions

This is a single-authored article.

Availability of data

Data can be obtained from the corresponding author upon reasonable request.

References

1. United Nations, Department of Economic and Social Affairs, Population Division. *World Urbanization Prospects: The 2018 Revision*. New York: United Nations; 2019.
2. Voogt JA, Oke TR. Thermal remote sensing of Urban climates. *Remote Sens Environ*. 2003;86(3):370-384. doi: 10.1016/S0034-4257(03)00079-8
3. Zhou W, Huang G, Cadenasso ML. Does spatial configuration matter? Understanding the effects of land cover pattern on land surface temperature in Urban landscapes. *Landsc Urban Plann*. 2011;102(1):54-63. doi: 10.1016/j.landurbplan.2011.03.009
4. Arnfield AJ. Two decades of Urban climate research: A review of turbulence, exchanges of energy and water, and the urban heat island. *Int J Climatol*. 2003;23(1):1-26. doi: 10.1002/joc.859

5. Akbari H, Pomerantz M, Taha H. Cool surfaces and shade trees to reduce energy use and improve air quality in Urban areas. *Sol Energy*. 2001;70(3):295-310. doi: 10.1016/S0038-092X(00)00089-X
6. Santamouris M. Cooling the cities-a review of reflective and green roof mitigation technologies to fight heat island and improve comfort in urban environments. *Sol Energy*. 2014;103:682-703. doi: 10.1016/j.solener.2012.07.003
7. Stewart ID, Oke TR. Local climate zones for Urban temperature studies. *Bull Am Meteorol Soc*. 2012;93(12):1879-1900. doi: 10.1175/BAMS-D-11-00019.1
8. Oke TR. City size and the Urban heat Island. *Atmos Environ*. 1973;7(8):769-779. doi: 10.1016/0004-6981(73)90140-6
9. Sobrino JA, Jiménez-Muñoz JC, Paolini L. Land surface temperature retrieval from LANDSAT TM 5. *Remote Sens Environ*. 2004;90:434-440. doi: 10.1016/j.rse.2004.02.003
10. Weng Q. Thermal infrared remote sensing for Urban climate and environmental studies: Methods, applications, and trends. *ISPRS J Photogramm Remote Sens*. 2009;64(4):335-344. doi: 10.1016/j.isprsjprs.2009.03.007
11. Chakraborty T, Lee X. A simplified Urban-extent algorithm to characterize surface Urban heat islands on a global scale and examine vegetation control on their spatiotemporal variability. *Int J Appl Earth Obs Geoinf*. 2019;74:269-280. doi: 10.1016/j.jag.2018.09.015
12. Zhou D, Xiao J, Bonafoni S, *et al*. Satellite remote sensing of surface urban heat islands: Progress, challenges, and perspectives. *Remote Sens*. 2019;11(1):48. doi: 10.3390/rs11010048
13. Carlson TN, Ripley DA. On the relation between NDVI, fractional vegetation cover, and leaf area index. *Remote Sens Environ*. 1997;62(3):241-252. doi: 10.1016/S0034-4257(97)00104-1
14. Keeratikasikorn C, Bonafoni S. Urban heat island analysis over the land use zoning plan of Bangkok by means of Landsat 8 imagery. *Remote Sens*. 2018;10(3):440. doi: 10.3390/rs10030440
15. Mallick J, Rahman A, Singh CK. Modelling urban heat islands in heterogeneous land surface and its correlation with impervious surface area by using night-time ASTER satellite data in highly urbanizing city, Delhi-India. *Adv Space Res*. 2013;52(4):639-655. doi: 10.1016/j.asr.2013.04.025
16. Wang W, Liu K, Tang R, Wang S. Remote sensing image-based analysis of the Urban heat island effect in Shenzhen, China. *Phys Chem Earth A B C*. 2019;110:168-175. doi: 10.1016/j.pce.2019.01.002
17. Katzschner A, Schwartze F, Thanh B, Schmid M. Introduction to Ho Chi Minh City. In: Katzschner A, Waibel M, Schwede D, Katzschner L, Schmid M, Storch H, editors. *Sustainable Ho Chi Minh City: Climate Policies for Emerging Mega Cities*. Berlin: Springer International Publishing; 2016. p. 5-17.
18. General Statistics Office. *Statistical Yearbook of Viet Nam 2022*. Wiley: Statistical Publishing House; 2022.
19. Anh NH, Trang NTD, Nguyen NTT, Trong TV, Son TV. Application of remote sensing of Ho Chi Minh city's surface temperature in period 2016-2020. *J Hydro Meteorol*. 2021;729:29-39. doi: 10.36335/VNJHM.2021(729).41-51
20. Li X, Zhou Y, Asrar GR, Imhoff M, Li X. The surface urban heat island response to Urban expansion: A panel analysis for the conterminous United States. *Sci Total Environ*. 2017;605-606:426-435. doi: 10.1016/j.scitotenv.2017.06.229
21. U.S. Geological Survey. *EarthExplorer*. Available from: https://earthexplorer.usgs.gov [Last accessed on 2024 Jun 05].
22. Chander G, Markham BL, Helder DL. Summary of current radiometric calibration coefficients for Landsat MSS, TM, ETM+, and EO-1 ALI sensors. *Remote Sens Environ*. 2009;113(5):893-903. doi: 10.1016/j.rse.2009.01.007
23. Ihlen V. *Landsat 8 Data Users Handbook*. USA: Department of the Interior U.S. Geological Survey; 2019.
24. Fallmann J, Forkel R, Emeis S. Secondary effects of Urban heat island mitigation measures on air quality. *Atmos Environ*. 2016;125:199-211. doi: 10.1016/j.atmosenv.2015.10.094
25. Rouse JW, Haas RH, Schell JA, Deering DW. *Monitoring Vegetation Systems in the Great Plains with ERTS. NASA. Goddard Space Flight Center 3d ERTS-1 Symposium*. Vol. 1. United States: NASA; 1974. p. 309-317.
26. Naim MNH, Kafy AA. Assessment of Urban thermal field variance index and defining the relationship between land cover and surface temperature in Chattogram city: A remote sensing and statistical approach. *Environ Challen*. 2021;4:100107. doi: 10.1016/j.envc.2021.100107
27. García DH, Díaz JA. Modeling the surface Urban heat island (SUHI) to study of its relationship with variations in the thermal field and with the indices of land use in the metropolitan area of Granada (Spain). *Sustain Cities Soc*. 2022;87:104166. doi: 10.1016/j.scs.2022.104166
28. Zhang Y, Yu T, Gu XF, *et al*. Land surface temperature retrieval from CBERS-02 IRMSS thermal infrared data and its applications in quantitative analysis of Urban heat island effect. *J Remote Sens*. 2006;10(5):789-797. doi: 10.11834/jrs.200605117
29. Peng S, Piao S, Ciais P, *et al*. Surface Urban heat island across 419 global big cities. *Environ Sci Technol*. 2012;46(2):696-703. doi: 10.1021/es2030438
30. Takebayashi H, Moriyama M. Surface heat budget on

green roof and high reflection roof for mitigation of Urban heat island. *Build Environ*. 2007;42(8):2971-2979. doi: 10.1016/j.buildenv.2006.06.017

31. Bowler DE, Buyung-Ali L, Knight TM, Pullin AS. Urban greening to cool towns and cities: A systematic review of the empirical evidence. *Landsc Urban Plann*. 2010;97(3):147-155. doi: 10.1016/j.landurbplan.2010.05.006
32. Santamouris M. Regulating the damaged thermostat of the cities: The increasing story of the Urban heat island. *Energy Build*. 2015;91(2):1-4. doi: 10.1016/j.enbuild.2015.01.027
33. Tan J, Zheng Y, Tang X, *et al*. The Urban heat island and its impact on heat waves and human health in Shanghai. *Int J Biometeorol*. 2010;54(1):75-84. doi: 10.1007/s00484-009-0256-x
34. Akbari H, Kolokotsa D. Three decades of Urban heat islands and mitigation technologies research. *Energy Build*. 2016;133:834-842. doi: 10.1016/j.enbuild.2016.09.067